Electron spin resonance in a two-dimensional electron gas induced by current or by electric field

Zbysław Wilamowski,[1,2,3] Włodzimierz Ungier,[1] and Wolfgang Jantsch[2]
[1]*Institute of Physics, Polish Academy of Sciences, Aleja Lotnikow 32/46, 02-668 Warszawa, Poland*
[2]*Institute of Semiconductor and Solid State Physics, Johannes Kepler Universität, A-4040 Linz, Austria*
[3]*Faculty of Mathematics and Computer Sciences, UWM Olsztyn, 10-561 Olsztyn, Poland*
(Received 15 July 2008; published 21 November 2008)

In asymmetric quantum wells an electric current induces an effective magnetic field acting on conduction electrons due to spin-orbit interaction. A high-frequency electric current can thus induce spin precession. We present and analyze a model for this current-induced (CI) electron spin resonance (ESR). In the low-frequency range, in high-mobility two-dimensional layers, CI ESR is the dominant mechanism of spin excitation. In the high-frequency limit, when the displacement current dominates, the drift current and momentum dissipation become irrelevant. There the CI ESR becomes equivalent to the well-known electric-dipole spin resonance. We show that in both limits the line shape of the power absorption spectra is described by the imaginary component of the dynamic magnetic susceptibility in contrast to experiment, indicative of another so far unknown mechanism.

DOI: 10.1103/PhysRevB.78.174423 PACS number(s): 76.30.−v, 71.70.Ej, 72.25.Pn, 72.25.Rb

I. INTRODUCTION

The mechanism of electric-dipole (ED) spin resonance (ED ESR) is well known for many years. It was theoretically predicted by Rashba and co-workers[1–4] and experimentally verified in various types of semiconductors and semimetals.[2,5] A specific dependence of the resonance amplitude on the direction of the microwave electric field is considered as an indicator, allowing one to distinguish electron spin resonance (ESR) excited by the electric field from the classical magnetic-dipole (MD) resonance excited by the microwave rf magnetic field since the latter type of resonance depends only weakly on the experimental geometry.

The theoretical modeling of electric-dipole ESR (ED ESR) is based on the analysis of the matrix element for electric-dipole transitions between spin states, which does not vanish because of the admixture of excited states due to spin-orbit coupling. Consequently, this type of resonance is called *electric-dipole spin resonance* with the acronym EDSR. Unfortunately the same acronym is also used for *electrically detected spin resonance*. These two acronyms are not equivalent: the first one stands for an excitation mechanism while the other one designates a method for detection. In this paper, we discuss the excitation mechanism by the microwave electric field. We show that, depending on electron mobility and the applied frequency, one can distinguish two excitation mechanisms. We shall call the electric-dipole spin resonance, as defined by Rashba, "ED ESR." For low mobility, a similar type of resonance occurs which is also induced by the electric field. At this type, momentum dissipation affects the excitation efficiency. We refer to it by "current-induced (CI) ESR" (CI ESR). The classical spin resonance is called the magnetic-dipole ESR (MD ESR) throughout this paper.

Excitation of ESR by an electric field experimentally is well verified in Si quantum wells.[6] First of all, ESR is easily detectable in spite of a rather small number of spins in the sample, and thus, not only ESR but also spin echoes could be observed.[7] The resonance has been also found in an array of quantum dots with weak lateral confinement showing signatures of spin-orbit interaction of the Rashba-type.[8] The high signal amplitude in both types of structures indicates that the effective spin-orbit field is much stronger than the magnetic component of the microwave field. In addition, there is a strong specific anisotropy of the ESR signal which constitutes another attribute of a resonance induced by the electric field.

In the traditional description of ED ESR,[1] energy dissipation due to momentum scattering is not taken into consideration. We argue here that such a model is limited to the high-frequency range, $\omega\tau_p \gg 1$. There the electric field oscillates many times during the time between two scattering events, τ_p. Therefore the ED transitions are hardly affected by the electron mobility.

The predictions of the ED ESR model are, however, in contrast to some experimental observations in semiconductors if $\omega\tau_p < 1$, particularly in two-dimensional (2D) layers.[9–12] Schulte *et al.*[13] showed that the resonance amplitude depends on the electron mobility. The quantitative analysis of the temperature dependence of the CI ESR indicates that the signal amplitude scales with the square of the electron mobility.[14] The observation that a dc electric current, due to spin-orbit coupling, which leads to the occurrence of an effective spin-orbit field acting on the electron spins,[6] helped in understanding the mechanism of the resonance excitation of high-mobility carriers. This effect shows that in this limit the resonance excitation is induced rather by the electric current than by the electric field in contrast to ED ESR.[3,4]

The concept of the CI ESR (Refs. 6 and 14) differs from that of ED ESR. We argue that the difference between CI and ED ESRs reflects the difference between drift and displacement currents. The driving force in CI ESR turns out to be frequency independent but proportional to the mobility-dependent current. In ED ESR, in contrast, the driving force is independent of the momentum scattering rate but it is expected to decrease with frequency. A diagrammatic treatment for the ESR excitation for 2D conduction electrons was presented by Duckheim and Loss.[15] For a specific geometry,

they analyzed the precession of the magnetic moment in the presence of spin-orbit interaction and disorder. They showed that spin-orbit interaction causes a broadening of the resonance linewidth. The excitation of spin transitions induced by an rf electric field leads also to spin currents. Disorder, which leads to momentum scattering, modifies ED ESR and causes motional narrowing of the resonance linewidth, i.e., the so-called Dyakonov-Perel spin relaxation.[16] This mechanism has been described also in the presence of cyclotron motion,[17] and it is experimentally well evidenced[11] but the problem of the resonance excitation by the spin-orbit field still requires further analysis.

In this paper, we discuss the specific selection rules of CI ESR showing that in contrast to MD ESR, the amplitude of CI ESR is strongly anisotropic. The selection rules for CI ESR are similar to those of ED ESR. We show that the ESR power absorption caused by the rf electric field can be expressed by a contribution to the electric conductivity which is proportional to the imaginary, i.e., the absorption part of the dynamic magnetic susceptibility. As long as the traditional spin-lattice relaxation of the absorbed power is assumed, all discussed types of ESR excitations, i.e., the effects of the real and the spin-orbit-like rf magnetic fields, lead to an absorption line shape only. The analyzed mechanisms, in spite of the complex interplay of the phase shifts, do not lead to a dispersive component of the ESR signal shape, which is in clear contrast to experiment.[11,18] Obviously, explanation of the latter requires consideration of an additional so far unidentified mechanism. Finally, we consider also the efficiency in exciting spin precession by an rf electric field for arbitrary geometry.

II. BYCHKOV-RASHBA FIELD

A. Effect of a direct current

In the presence of "structure inversion asymmetry,"[19] e.g., in samples with asymmetric quantum wells (due to the presence of different interfaces or a perpendicular electric field), spin splitting may occur already without external magnetic field. This effect can be ascribed to an effective magnetic field, which is called now the Bychkov-Rashba (BR) field, $\mathbf{H}_{\mathrm{BR}}$,

$$g\mu_0\mu_B\mathbf{H}_{\mathrm{BR}} = a_{\mathrm{BR}}(\mathbf{k}\times\mathbf{n}), \tag{1}$$

where g is the g factor, μ_B the Bohr magneton, and $\mathbf{n}$ is a unit vector describing the direction in which the symmetry is broken.[19] The phenomenological parameter a_{BR} depends on the strength of spin-orbit interaction and interface details.[20,21]

Experimentally, Kalevich and Korenev[22] observed Hanle depolarization when they applied a dc current to a two-dimensional electron gas (2DEG) at the GaAs/AlGaAs interface. They attributed this to a mean spin-orbit field induced by the current. They also suggested that this field might be detectable as a shift of the resonance in an ESR experiment. This effect has been observed recently on Si quantum wells in between SiGe barriers.[6] Such samples, when modulation doped, exhibit low-temperature mobilities up to 600.000 $\mathrm{cm}^2/\mathrm{V\,s}$. High mobilities can be achieved only in samples doped with donors in the upper barrier, and therefore, the quantum well experiences a static perpendicular electric field that lowers the symmetry. The lower symmetry allows for the Bychkov-Rashba field.

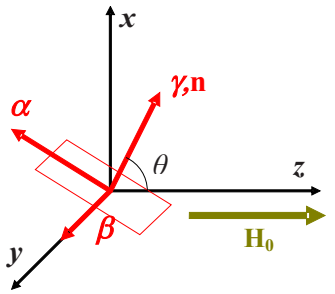

FIG. 1. (Color online) Coordinate system used: the sample normal $\mathbf{n}$ is tilted with respect to the static magnetic field, $\mathbf{H}_0$, by an angle θ. A new coordinate system, α,β,γ, is used which is anchored to the sample. The 2D sample is indicated by a rectangle.

It has been shown that a finite mean effective spin-orbit field, δH_{BR}, results from the momentum ($\hbar\mathbf{k}$)-dependent BR spin splitting, $\hbar\boldsymbol{\omega}_{\mathrm{BR}}=a_{\mathrm{BR}}[\mathbf{k}\times\mathbf{n}]$, of individual electrons and the drift velocity,[6] $\mathbf{v}_d$,

$$\mu_0\delta\mathbf{H}_{\mathrm{BR}} = \beta_{\mathrm{BR}}(\mathbf{n}\times\mathbf{v}_d) = \frac{\beta_{\mathrm{BR}}}{n_s e}(\mathbf{n}\times\mathbf{j}). \tag{2}$$

Here $\mathbf{n}$ is the unit vector perpendicular to the sample layer, and the material parameter $\beta_{\mathrm{BR}}=a_{\mathrm{BR}}m^*/g\mu_B\hbar$ depends on the effective mass, m^*, and the sheet carrier density, n_s. Equation (2) shows that the BR field averaged over the 2D electron gas is proportional to the electric current, $\mathbf{j}$, and thus to the electron mobility.

The BR field, as described by Eq. (2), results from a shift of the Fermi circle in $\mathbf{k}$ space by the drift vector, $\mathbf{k}_d$. Because of the fast momentum scattering, (much faster than the spin dephasing rate, $1/T_2$), the BR field, which is seen by individual electrons, is well averaged by many scattering events. In Si/SiGe structures, the dephasing time is of the order of 1 μs while the momentum scattering time is of the order of $\tau_p \leq 1\times10^{-11}$ s. As a consequence, the precession of the total magnetic moment of the carrier spins can be affected by the average BR field. A dc current leads to a detuning of the resonance field while an rf component is expected to excite spin transitions by driving the precession.[6]

B. Radio-frequency Bychkov-Rashba field

If a conducting sample is placed in the microwave field then an in-plane electric microwave component causes an rf current which leads to an rf magnetic field that allows one to excite ESR. We choose a coordinate system, (x,y,z), related to the external magnetic-field vector, $\mathbf{H}_0=(0,0,H_0)$ (see Fig. 1). Since we want to discuss a general geometry we assume that the oscillating electric field in a microwave cavity, $\mathbf{E}(t)=\mathrm{Re}(\mathbf{E}e^{-i\omega t})$, can have any direction, $\mathbf{E}=(E_x,E_y,E_z)$, but all components oscillate with a common phase. Therefore, without loss of generality, we can assume that all compo-

nents of the electric field have only real values. In that way we can define the phase shifts of all other quantities relative to that of the oscillating electric-field vector.

The local 2D current density is described by the complex conductivity tensor in $\mathbf{j}=\hat{\sigma}(\omega)\mathbf{E}$. The real part of the complex conductivity stands for the drift current, which occurs in phase with the electric field, while the imaginary part corresponds to the displacement current.

For an arbitrary sample orientation, when the vector normal to the layer, $\mathbf{n}$, is tilted from the z direction by an angle θ, we choose another coordinate system, (α,β,γ), related to the sample layer in such way that $\mathbf{n}=\hat{\gamma}$ is in the (x,z) plane, i.e., $\mathbf{n}=(\sin\theta,0,\cos\theta)$. Moreover, since the in-plane crystallographic axes do not play any role for Si, we assume that $\hat{\beta}$ and $\hat{y}$ coincide. Consequently, the α axis has the components $\hat{\alpha}=(\cos\theta,0,-\sin\theta)$ in the (x,y,z) coordinate system.

Within the coordinate system related to the sample axes, (α,β,γ), the transverse component of the current (perpendicular to the 2D electron system) can be neglected,[4] $j_\gamma=0$, and the in-plane components of the conductivity tensors have the well known forms. They can be described by the frequency-dependent longitudinal components, $\sigma_{\alpha\alpha}=\sigma_{\beta\beta}$, and the Hall conductivity $\sigma_{\alpha\beta}=-\sigma_{\beta\alpha}$ components of the conductivity tensor.

For the discussion of the current-induced ESR it is convenient to define conductivities $\sigma_\pm$ corresponding to the cyclotron active and cyclotron inactive components. Within the Drude model (omitting Landau quantization) we have

$$\sigma_\pm=\sigma_{\alpha\alpha}\pm i\sigma_{\alpha\beta}=\frac{n_s e^2\tau_p}{m^*}\frac{1}{1-i(\omega\pm\omega_c)\tau_p}\equiv\frac{n_s e^2\tau_\pm}{m^*}, \tag{3}$$

where ω_c is the cyclotron frequency $\omega_c=e\mu_0 H_0|\cos\theta|/m^*$. For simplification we introduced here

$$\tau_\pm=\frac{\tau_p}{1-i(\omega\pm\omega_c)\tau_p}. \tag{4}$$

For $\omega\tau_p\ll 1$, this characteristic time approaches $\tau_\pm\to\tau_p$, while in the high frequency limit (when $\omega\tau_p\gg 1$) $\tau_\pm\to i/(\omega\pm\omega_c)$.

From Eqs. (2)–(4) one can find the dependence of the BR field on the magnitude of the microwave electric field. To distinguish ESR active and inactive components of the oscillating fields, we introduce a coordinate system rotating around the applied magnetic field, H_0, where the right- and left-hand rotating axes are $\hat{a}_\pm=(\hat{x}\pm i\hat{y})/\sqrt{2}$. Within such coordinates the ESR active and inactive components of the BR field are

$$\mu_0 H_{\mathrm{BR}\pm}=\mp\frac{\beta_{\mathrm{BR}}e}{m^*}\mathbf{T}_\pm\cdot\mathbf{E}, \tag{5}$$

where

$$\mathbf{T}_\pm=\frac{1}{2}\begin{bmatrix} i[\tau_+(1\pm\cos\theta)+\tau_-(1\mp\cos\theta)]\cos\theta \\ \tau_+(1\pm\cos\theta)-\tau_-(1\mp\cos\theta) \\ -i[\tau_+(1\pm\cos\theta)+\tau_-(1\mp\cos\theta)]\sin\theta \end{bmatrix}, \tag{6}$$

is a time vector relating the BR field and the microwave electric field.

As it is shown below in Sec. III the driving force of ESR and the Rabi frequency are determined by the modulus $|H_{\mathrm{BR}\pm}|$.

Equation (5) is the general expression describing the driving field for the precession of the sample magnetization, which is caused by an electric field. The discussion of the properties of the rf BR field becomes much more transparent when a specific experimental geometry is assumed. Below we discuss the case when the electric field is parallel to the external magnetic field, $\mathbf{E}=(0,0,E_z)$. This is the case for a rectangular TE_{201} microwave cavity which is commonly used in standard ESR spectrometers.

1. Current-induced and electric-dipole electron spin resonances

When the sample layer is oriented such that the electric field is in plane, the vector $\mathbf{n}$ is oriented along the x axis, and $\mathbf{n}=(1,0,0)$, i.e., $\theta=90°$ and $\omega_c=0$, and consequently $\tau_+=\tau_-=\tau_p$. In that case, the expressions for the BR field take a very simple form which allows one to easily distinguish CI and ED ESRs. According to Eqs. (5) and (6) the BR fields for this geometry are

$$\mu_0 H_{\mathrm{BR}\pm}=\pm\frac{i\beta_{\mathrm{BR}}eE_z}{m^*}\frac{\tau_p}{1-i\omega\tau_p}. \tag{7}$$

A similar case was discussed by Duckheim and Loss.[15] The driving force for the ESR and also the Rabi frequency are described by the modulus of the BR field,

$$\mu_0|H_{\mathrm{BR}\pm}|=\frac{\beta_{\mathrm{BR}}eE_z}{m^*}\frac{\tau_p}{\sqrt{1+\omega^2\tau_p^2}}. \tag{8}$$

The dependence of $\mu_0|H_{\mathrm{BR}\pm}|$ normalized by $\frac{\beta_{\mathrm{BR}}eE_z}{m^*}$ is plotted in Fig. 2 as a function of frequency.

One can distinguish two different limits. For $\omega\tau_p\ll 1$, the current follows changes of the electric field, and Eq. (8) takes the form $\mu_0|H_{\mathrm{BR}\pm}|=\frac{a_{\mathrm{BR}}eE_z\tau_p}{g\mu_B\hbar}$. The driving field does not depend on frequency, it is proportional to the spin-orbit coupling and scales with the momentum relaxation time, i.e., with the electron mobility. Therefore it is the current which rules the resonance excitation, and thus, we call this CI ESR.

For the high-frequency range, $\omega\tau\gg 1$, the driving force $\mu_0|H_{\mathrm{BR}\pm}|=\frac{\beta_{\mathrm{BR}}eE_z}{m^*\omega}=\frac{a_{\mathrm{BR}}eE_z}{g\mu_B\hbar\omega}$ is mobility and mass independent and it is inversely proportional to the frequency. This is the case of ED ESR discussed by Rashba and co-workers.[2–4] CI ESR emerges from ED ESR when momentum relaxation leads to a damping of the driving force in the latter. On the other hand, ED ESR may be derived from CI ESR at high frequency when the mobility-dependent drift current tends to the mobility-independent displacement current.

For a comparison of the efficiency of the CI ESR with the classical MD ESR, the dash-dotted line in Fig. 2 shows the microwave magnetic field, H_1, responsible for the direct MD

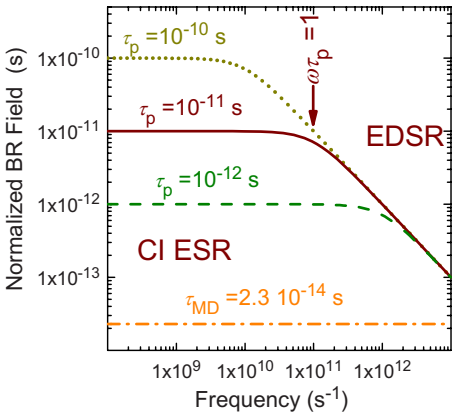

FIG. 2. (Color online) Frequency dependence of the driving field, $|H_{\mathrm{BR}+}|$, normalized by $\beta_{\mathrm{BR}}eE_z/m^*$ for various momentum relaxation times, τ_p [Eq. (8)]. The dash-dotted line corresponds to the maximum value of the (normalized) microwave field, H_1, at its antinode, where the β_{BR} value is that of a Si layer. For the other curves E_1^0 is taken at the node of H_1.

transitions. Both H_{BR} and the magnetic component of the microwave field, H_1, are normalized by the same factor, $\beta_{\mathrm{BR}}eE_x/m^*$, using parameters for Si. The ratio $E_1^0/\mu_0 H_1^0 = c$ has been taken for the empty cavity, i.e., both screening of H_1 by eddy currents and the modification of E_1 by lattice and charge polarizations have been neglected. For high electron mobility, CI excitation exceeds the MD mechanism in efficiency. In particular, for a Si/SiGe layer, where the mobility reaches values of a few times 1×10^5 cm^2/V s, the momentum relaxation time ($\tau_p \approx 3\times10^{-11}$ s) is by three orders of magnitude longer than the characteristic time $\tau_{\mathrm{MD}} = g\mu_B\hbar/a_{\mathrm{BR}}ec = 2.3\times10^{-14}$ s, where CI and MD transitions are equally probable. For high-mobility samples, the graph shows that the spin-orbit field exceeds the microwave magnetic field by more than three orders of magnitude. In view of the very weak spin-orbit coupling of Si, one can expect that for III-V semiconductors τ_{MD} is even shorter, and the CI efficiency is even more pronounced.

2. Angular dependence of CI ESR

In the low-frequency limit, $\omega\tau_p \ll 1$, the cyclotron resonance is damped by momentum scattering, $\tau_\pm \to \tau_p$, and the time vector, as defined by Eq. (6), tends to

$$\mathbf{T}_\pm \to \tau_p \begin{bmatrix} i\cos\theta, \\ \pm\cos\theta, \\ -i\sin\theta \end{bmatrix}. \tag{9}$$

The modulus of the BR field is given by the following expression:

$$\mu_0|H_{\mathrm{BR}\pm}|_{\mathrm{CI}} = \frac{\beta_{\mathrm{BR}}e\tau_p}{m^*}[(E_x^2+E_y^2)\cos^2\theta + E_z^2\sin^2\theta - E_xE_z\sin 2\theta]^{1/2}. \tag{10}$$

For the electric microwave field oriented parallel to the external magnetic field, the BR field scales with the in-plane component of the microwave electric field

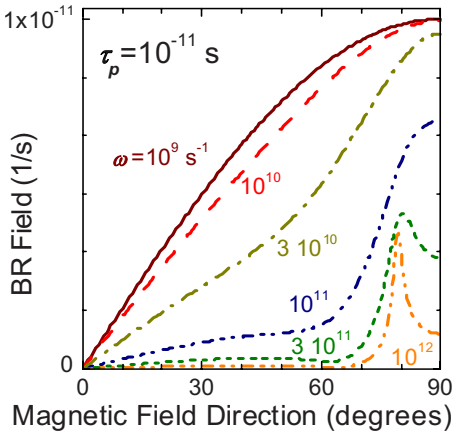

FIG. 3. (Color online) Dependence of the BR field (normalized as in Fig. 2) on the sample orientation, as described by the modulus of Eq. (12).

$$\mu_0|H_{\mathrm{BR}\pm}|_{\mathrm{CI}} = \frac{\beta_{\mathrm{BR}}e\tau_p}{m^*}E_z|\sin\theta|. \tag{11}$$

The induced current is directed along the sample plane, which is parallel to the (x,z) plane. Consequently, $\mathbf{H}_{\mathrm{BR}}$, is parallel to the y direction and perpendicular to the applied field.

3. Influence of cyclotron motion on CI and ED ESRs

When $\omega\tau_p \geq 1$ and the external static magnetic field has a component perpendicular to the sample layer, the cyclotron motion has to be taken into account.[11] If the electric microwave field is oriented along the z axis, $\mathbf{E}=(0,0,E_z)$, and the normal to the sample is tilted by an angle θ, $\mathbf{n}=(\sin\theta,0,\cos\theta)$, then Eqs. (6) and (7) give

$$\mu_0 H_{\mathrm{BR}\pm} = \pm\frac{i\beta_{\mathrm{BR}}e}{m^*}\frac{\tau_p}{2}\left[\frac{(1\pm\cos\theta)}{1-i(\omega+\omega_c)\tau_p} + \frac{(1\mp\cos\theta)}{1-i(\omega-\omega_c)\tau_p}\right]E_z\sin\theta. \tag{12}$$

The modulus of $\mu_0 H_{\mathrm{BR}+}$, normalized by $\beta_{\mathrm{BR}}eE_z/m^*$, is plotted in Fig. 3 as a function of the angle θ. Results are given for $\tau_p = 1\times10^{-11}$ s and different frequencies. The values for $\theta = 90°$ correspond to the dependence shown in Fig. 2. The solid line for small frequency, $\omega = 1\times10^9$ s^{-1}, corresponds to a pure CI ESR, as described by Eq. (11). When the parameter $\omega\tau_p$ increases, a maximum appears close to $\theta \cong 80°$. For that orientation the cyclotron and the spin precession frequencies are equal. At the cyclotron resonance the carrier velocity is enhanced, which leads also to a resonant increase in the BR field.

For high frequency, ($\omega\tau_p \gg 1$), the case described by Eq. (12) tends to the results of Rashba and Efros.[3,4] The matrix element occurs to be independent of τ_p and scales with $\omega/(\omega_c^2-\omega^2)$. In the low-frequency limit, where the cyclotron motion is effectively quenched, the solution becomes independent of the cyclotron frequency, ω_c. There it tends toward the dependence described by Eq. (11).

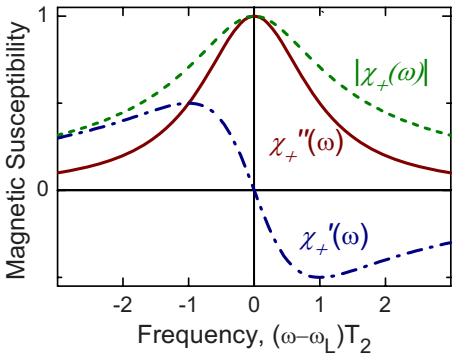

FIG. 4. (Color online) Components of the magnetic susceptibility as a function of the normalized frequency. Dashed line: modulus of the susceptibility, $|\chi_+(\omega)|$, describing the amplitude of the precessing magnetization [Eq. (15)]. Dashed-doted line: real part of the susceptibility which describes the amplitude of the magnetization occurring in phase with the effective rf magnetic field [Eq. (14)]. Solid line: imaginary part of the susceptibility, $\chi''(\omega)$. The latter curves represent the amplitude of the out-of-phase magnetization and the spectrum of the power absorption, respectively.

III. RESONANCE EXCITATION

The spin precession in a static magnetic field, $\mathbf{H}_0$, and the oscillating BR field, $\mu_0\mathbf{H}_{\mathrm{BR}}(t)$, are described by the well-known Bloch equations.[23] Here in the driving field $\mathbf{H}_{\mathrm{BR}}$ has to be included. As a result of $\mathbf{H_0}$, the magnetic moment, $\mathbf{M}$, precesses with the Larmor frequency, $\boldsymbol{\omega}_L=\gamma_B\mu_0\mathbf{H_0}$, where $\gamma_B=g\mu_B/\hbar=\gamma_H/\mu_0$ is the gyroscopic factor.

Two solutions of the Bloch equations are usually discussed. For strong excitation, the magnetization vector precesses around both the external magnetic field and the direction of $\mathbf{H}_{\mathrm{BR}}$. For the latter precession, the z component of magnetization, $M_z=M_0e^{-i\omega_R t}$, oscillates with the Rabi frequency $\omega_R=\gamma_B|\mu_0H_{\mathrm{BR}}|$. For weak, continuous excitation, however, the magnetization reaches a steady-state equilibrium. The solution of the Bloch equations shows that here the Rabi precession is excited by the components of the oscillating BR field which are transverse to $\mathbf{H_0}$.

In the rotating coordinate system, the amplitudes of right- and left-hand rotating components of the magnetization, $M_\pm=(M_x\mp iM_y)/\sqrt{2}$, are described by the linearized solution of the Bloch equations,

$$M_\pm=\chi_\pm(\omega)H_{\mathrm{BR}\pm}, \tag{13}$$

where the real (dispersive) and imaginary (absorption) parts of the susceptibility are expressed by

$$\chi'_\pm(\omega)=\mu_0\pi\gamma_BM_0\frac{1}{\pi}\frac{(\omega_L\mp\omega)T_2^2}{1+(\omega_L\mp\omega)^2T_2^2},$$

$$\chi''_\pm(\omega)=\pm\mu_0\pi\gamma_BM_0\frac{1}{\pi}\frac{T_2}{1+(\omega_L\mp\omega)^2T_2^2}. \tag{14}$$

Both are plotted in Fig. 4. The absorption part $\chi''_\pm(\omega)=\pm\mu_0\pi\gamma_BM_0f_L(\pm\omega)$ is described by the Lorentz shape function: $f_L(\omega)=\frac{1}{\pi}\frac{T_2}{1+(\omega_L-\omega)^2T_2^2}$. For a long spin-relaxation time, $\omega_LT_2\gg1$, only one of the rotating components, $H_\pm$, effectively excites ESR. In particular, for a positive g factor, i.e., a positive Larmor frequency, the right-hand rotating component, H_+, is ESR active.

The amplitude of the precession, $|M_\pm|$, is obtained by $|M_\pm|=|\chi_\pm||H_\pm|$. Therefore $|H_\pm|$ can be treated as a driving force of the ESR. The modulus of the dynamic susceptibility is described by

$$|\chi_\pm(\omega)|=\mu_0\pi\gamma_BM_0\frac{1}{\pi}\frac{T_2}{\sqrt{1+(\omega_L\mp\omega)^2T_2^2}}$$

$$=\mu_0\pi\gamma_BM_0\sqrt{\frac{T_2}{\pi}}\sqrt{f_L(\pm\omega)}, \tag{15}$$

and the phase shift between the transverse components of the field and the magnetization, φ_{HM}, is frequency dependent and changes its sign at the resonance condition according to $\tan\varphi_{MH}=\pm(\omega_L\mp\omega)T_2$ (see also Fig. 4).

The two-dimensional Pauli magnetization is given by

$$M_0=g\mu_Bsn_P=g\mu_Bs\frac{1}{2}\hbar\omega_LD_s=g\mu_Bs\hbar\omega_L\frac{g_s}{2}\frac{g_vm^*}{\pi\hbar^2}, \tag{16}$$

where the sheet concentration of uncompensated spins is $n_p=\hbar\omega_LD_s/2$ for the low-temperature range, $s=1/2$ stands for the electron spin, and D_s is the density of states for both spin subbands (for strained Si layers the valley degeneracy factor is $g_v=2$). The sheet electron concentration is: $n_s=D_sE_F$ and the ratio $\frac{n_P}{n_c}=\frac{1}{2}\frac{\hbar\omega}{E_F}$.

IV. POWER ABSORPTION

A. Line shape of the power absorption spectra

The microwave power absorbed by the magnetic moment $\mathbf{M}(t)$ in an oscillating magnetic field is given by the general formula[24]

$$P_M=-\frac{\mu_0}{T}\int_0^T\mathbf{M}(t)\frac{d\mathbf{H}(t)}{dt}dt. \tag{17}$$

For the case of a 2D layer, where the 2D magnetization is described by Eqs. (13)–(15), the power absorbed per unit area is

$$\frac{dP_M}{dA}=\frac{1}{2}\mu_0\omega\chi''_+(\omega)|H_{\mathrm{BR}+}|^2+\frac{1}{2}\mu_0\omega\chi''_-(\omega)|H_{\mathrm{BR}-}|^2. \tag{18}$$

The absorbed power is, thus, proportional to the imaginary part of the dynamic magnetic susceptibility and the square of the amplitude of the rf BR field.

The modulus $|H_{\mathrm{BR}+}|$ can be treated as a driving force of ESR. It determines the Rabi frequency and the amplitude of the oscillating component of magnetization. The square of $|H_{\mathrm{BR}+}|^2$ rules the power absorption, i.e., the amplitude of ESR absorption signals.

In the case of ESR excitation by electric fields and spin-orbit coupling, there is a complex interplay of the directions and phases of oscillating quantities. The power absorbed by the magnetic system leads to a tilting of the magnetic moment from the direction of the external field, and it is deter-

mined only by the relation between the rf field, $\mathbf{H}(t)$, and the magnetization, $\mathbf{M}(t)$, according to Eq. (17). However, as long as this relation can be derived by the Bloch equations the expression for the power absorption [see Eq. (18)] is a general expression for the spin resonance absorption signal, which is independent of the origin of the effective rf fields. Consequently, the absorption line shape is expected also in the case when spins are excited by the simultaneous effect of microwave magnetic field and the spin-orbit field, $\mathbf{H}(t) = \mathbf{H}_1(t) + \mathbf{H}_{\mathrm{BR}}(t)$, which can be arbitrarily directed and shifted in phase.[14]

For a 2D system, the line asymmetry reflecting the occurrence of a dispersive component, $\chi'_{\pm}(\omega)$, cannot be related to the Dyson effect,[25] which is common in bulk metals. Therefore the fact that a dispersive component is observed in the power absorption spectrum[6,11] indicates that one has to consider another mechanism of spin-dependent power absorption and/or some specific spin-relaxation mechanisms, which cannot be described by a constant spin-relaxation rate. The latter is assumed, however, in deriving the Bloch equations.

B. Amplitude of the power absorption ESR signal

The amplitude of the ESR absorption signal induced by an rf electric field is described by Eq. (18) where the modulus of the BR field is given by Eqs. (5) and (6). The dependence of $|H_{\mathrm{BR}\pm}|$ on the experimental geometry, the frequency, and the momentum relaxation time is discussed in Sec. II.

For the specific geometry discussed in Sec. II B (electric microwave and external magnetic field are parallel and in-plane oriented). Eq. (18) takes the simpler form

$$\frac{dP_M}{dA} = \frac{1}{2}\left(\frac{\beta_{\mathrm{BR}} e E_z}{m^*}\right)^2 \frac{\omega\tau_p^2}{1+\omega^2\tau_p^2} \pi\gamma_B M_0 [f_L(\omega) - f_L(-\omega)]. \tag{19}$$

The integrated ESR signal amplitude, i.e., the precoefficient of the Lorentz shape function, is proportional to the square of the BR parameter. Since the static magnetization is proportional to the Larmor frequency [see Eqs. (15) and (16)] the nominator in Eq. (19) is proportional to the square of frequency (one factor ω comes from M_0) and the square of the momentum relaxation time. This dependence is plotted in Fig. 5. The high-frequency limit, $\omega\tau_p \gg 1$, corresponds to the limit of ED ESR. There the signal amplitude becomes independent of frequency and of the momentum relaxation time. In the low-frequency range corresponding to CI ESR, the signal scales with $\omega^2\tau_p^2$, showing the importance of the electron mobility. The dash-dotted line in Fig. 5 corresponds to the amplitude of MD ESR. The amplitude of MD ESR has been normalized for Si/SiGe material parameters in the same way as in Fig. 2. One can see that even for Si/SiGe structures, where spin-orbit coupling is weak, the efficiency of ESR excitation by an rf electric field can be by orders of magnitude more effective than the excitation by an rf magnetic microwave field. For $\tau_p \cong 1 \times 10^{-11}$ s in Si/SiGe, the CI ESR is, thus, expected to be by four orders of the magnitude bigger than MD ESR. For III-V materials, where spin-orbit coupling is stronger, the difference can be even more pronounced.

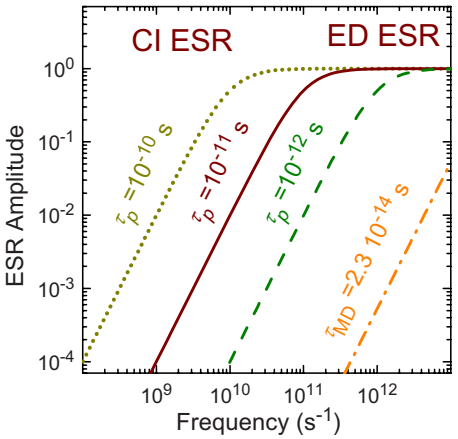

FIG. 5. (Color online) Dependence of the ESR absorption signal originating from the BR field as a function of frequency, where $\mathbf{E}_1$ and $\mathbf{H}_0$ are parallel to the z axis. The static magnetization has been assumed to be proportional to the Larmor frequency. The dash-dotted line corresponds to the amplitude of MD ESR (which is normalized in the same way as in Fig. 2).

One should also notice that in the very high-frequency limit (beyond the scale of Fig. 5), the MD ESR exceeds the amplitude of ED ESR. The MD ESR amplitude increases with frequency as a result of the derivative in Eq. (17) and of the increase in magnetization at the Larmor frequency. For the case of ED ESR, the increase is compensated by the decrease in the amplitude of the displacement current [see Eqs. (3) and (8)].

For an arbitrary sample orientation, when the normal to the sample layer is tilted with respect to the z direction by an angle θ ($\mathbf{E}$ and $\mathbf{H}_0$ are still assumed to be parallel to the z axis) the cyclotron motion takes place and the dependence of the signal amplitude on experimental geometry becomes more complex. Figure 6 shows the dependence of the ESR signal amplitude on θ, where the BR field is given by Eq. (12).

The enhancement of the signal amplitude, caused by an increase in the electron velocity at the cyclotron resonance, is well seen. It is well pronounced for $\omega\tau_p > 1$. It occurs for the sample orientation for which the cyclotron frequency coincides with the spin resonance frequency.

V. SPIN-DEPENDENT ELECTRIC CONDUCTIVITY

Equation (19) is the classical expression for the power absorbed by the spin system due to the rf magnetic field. In the case when this field originates from the rf electric field, $\mathbf{E}$, as described by Eq. (5), the expression can be rewritten in the form

$$\frac{dP_M}{dA} = \frac{1}{2\mu_0}\omega\left(\frac{\beta_{\mathrm{BR}} e}{m^*}\right)^2 [\chi''_+(\omega)|\mathbf{T}_+ \cdot \mathbf{E}|^2 + \chi''_-(\omega)|\mathbf{T}_- \cdot \mathbf{E}|^2], \tag{20}$$

which underlines the fact that the magnetic energy of spins in an external magnetic field is pumped by the rf electric field.

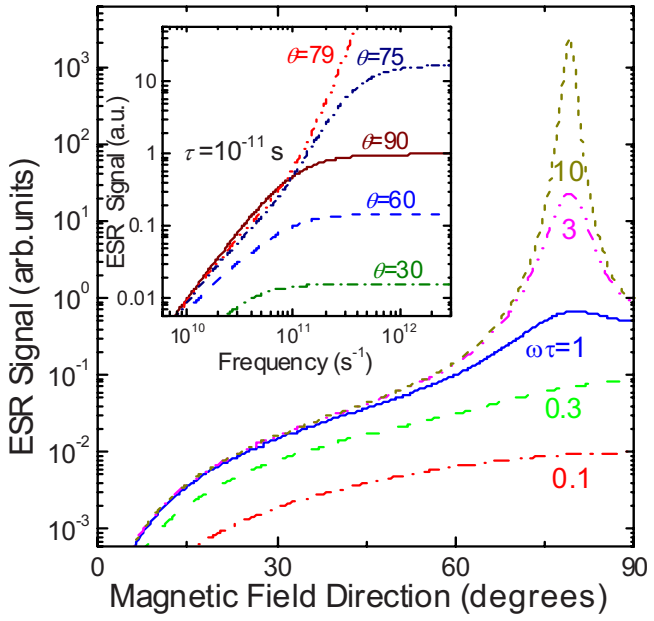

FIG. 6. (Color online) Dependence of the ESR signal induced by the microwave electric field on the tilt angle θ of the static magnetic field $\mathbf{H}_0$ relative to the vector $\mathbf{n}$. The inset shows the frequency dependence of the ESR signal for different angles θ.

Therefore, this contribution can be treated as a spin-dependent contribution to the rf electric conductivity,

$$\frac{dP_M}{dA} = \frac{1}{2}\mathrm{Re}(\mathbf{E}^* \hat{\sigma}_s \mathbf{E}), \tag{21}$$

where $\hat{\sigma}_s$ is a tensor.

Equation (21) shows already that measuring the rf conductivity, e.g., by monitoring the power absorbed by a sample placed in an rf electric field, allows one to detect ESR. In that sense, Eq. (21) describes one mechanism for the electrical detection of ESR. In fact, the spin contribution is proportional to the magnetic susceptibility, $\chi''(\omega)$. In the vicinity of the ESR condition, the components of $\mathbf{T}_\pm$ weakly depend on frequency and the spin-dependent part of the conductivity is proportional to the Lorentz shape function. But one has to underline that the discussed contribution to the electric power absorption differs in the kind of power dissipation from the classical Joule heat. The electric conductivity results from the dissipation of the electron momentum and its kinetic energy in the electron-scattering processes, while the power absorbed in the spin-dependent contribution is dissipated via the spin-relaxation channels.

In nonmagnetic semiconductors, the spin-dependent contribution to the total electric conductivity, σ, is small. Assuming a low-frequency Drude-type of electric conductivity, $\sigma = n_s e^2 \tau_p / m^*$, and in-plane orientation of $\mathbf{H}_0$ and $\mathbf{E}(t)$, the ratio of σ_s and σ becomes

$$\Phi_s(\omega) \equiv \frac{\sigma_s(\omega)}{\sigma} = \frac{\omega m^*}{\mu_0 n_s} \frac{\tau_p^2 \alpha_{\mathrm{BR}}^2}{g^2 \mu_B^2 \hbar^2} [\chi_+''(\omega) + \chi_-''(\omega)]. \tag{22}$$

This ratio depends on material parameters, and its frequency dependence is dominated by the shape function of ESR, $\chi_+''(\omega)$. For the case when the spin-relaxation time is dominated by the Dyakonov-Perel mechanism, which normally is the case of Si/SiGe structures,[10,11] the transverse spin-relaxation time is inversely proportional to the square of the BR parameter, to the sheet electron concentration, and to the momentum relaxation time: $T_2 = 2\hbar^2 / 3\alpha_{\mathrm{BR}}^2 \pi n_s \tau_p$. The dynamic susceptibility at the Larmor frequency, i.e., at the center of ESR, $\chi_+''(\omega_L)$, is proportional to T_2 [see Eq. (15)], and thus, the ratio (22) can be given by the simple expression

$$\Phi_s(\omega_L) = \frac{1}{6 g_v g_s} \left(\frac{\hbar \omega_L}{E_F} \right)^2. \tag{23}$$

Φ_s scales, thus, with the square of the ratio of spin splitting to the Fermi energy, indicating the important role of a spin-dependent conductivity in semiconductor structures with a small Fermi energy. For the Si/SiGe structures, where the sheet electron concentration is a few times 1×10^{11} cm^{-2}, we obtain, assuming a magnetic field of $B_0 \cong 0.3$ T (corresponding to an ESR frequency of about $\omega = 2\pi \times 9$ GHz), a ratio of $\Phi_s \cong 2 \times 10^{-5}$.

The spin contribution is, thus, small as compared to the total conductivity; nevertheless, the experimental detection of this component is relatively easy mainly because in the vicinity of ESR the dynamic susceptibility strongly depends on frequency. The detection is particularly easy when the magnetic field is modulated. Anyway, as it was discussed above, in Secs. II and IV (see Fig. 2), for high-mobility samples the spin-dependent contribution to the power absorption caused by BR coupling can be much bigger than the classical MD signal.

VI. CONCLUSIONS

In high-mobility systems, ESR excitation by current is much more efficient than by magnetic-dipole transitions. CI ESR is a form of ESR induced by electric-dipole transitions where damping of the electron motion leads to the reduction in the transition matrix element of EDSR by a factor $\omega\tau_p$. In this paper we discussed the efficiency of the resonance excitation and the resulting Rabi frequency by an rf electric field, and we evaluated one of the channels for the energy transfer. The sample temperature enters only via the momentum scattering time, $\tau_p(T)$, at least as long as we are dealing with degenerate statistics. The strong enhancement of the microwave magnetic field will be most pronounced, thus, at low temperatures where the mobility of the 2D electrons is highest. The microwave energy causes motion of carriers resulting in an effective spin-orbit magnetic field, which drains microwave energy to the spin system. In a classical picture, the energy of the spin system depends on the angle of the precession or, in the quantum-mechanical description, the population of the excited spin state. For weak excitation, in a steady state, the spin energy is transferred to the lattice via spin-lattice relaxation. For strong excitation, when the spin relaxation is not sufficiently effective, Rabi oscillations occur. In that case, they are equivalent to an energy oscillation back and forth between the spin reservoir and the microwave energy in the cavity.

We derived a generalized picture of the mechanism previously described by Rashba and Efros[3,4] and by Duckheim and Loss.[15] As it is shown here, this mechanism should result for a 2D system in an ESR signal with a pure absorption-like line shape, and the phase relation between the rf spin-orbit field and the precessing magnetization is exactly the same as in all other types of magnetic resonances which are described by the Bloch equations. Therefore, the experimentally observed line shape and the dependence of the ESR signal on the microwave power indicate that other channels of the energy transfer are spin dependent, leading to the occurrence of a dispersive component of the absorption signal and to the dependence of the rf electric conductivity on spin excitation, which results in the polarization signal observed earlier.[10,18,26,27]

ACKNOWLEDGMENTS

This work was supported in Austria by the *Fonds zur Foerderung der Wissenschaftlichen Forschung*, OeAD, and GMe (all Vienna) and in Poland by MNiSW under Project No. 2007-10.

[1] E. I. Rashba, Sov. Phys. Solid State **2**, 1109 (1960).
[2] E. I. Rashba and V. I. Sheka, in *Landau Level Spectroscopy*, edited by G. Landwehr and E. I. Rashba (North-Holland, Amsterdam, 1991), p. 131.
[3] E. I. Rashba and Al. L. Efros, Appl. Phys. Lett. **83**, 5295 (2003).
[4] Al. L. Efros and E. I. Rashba, Phys. Rev. B **73**, 165325 (2006).
[5] M. Dobrowolska, Y. F. Chen, J. K. Furdyna, and S. Rodriguez, Phys. Rev. Lett. **51**, 134 (1983).
[6] Z. Wilamowski, H. Malissa, F. Schäffler, and W. Jantsch, Phys. Rev. Lett. **98**, 187203 (2007).
[7] A. M. Tyryshkin, S. A. Lyon, W. Jantsch, and F. Schäffler, Phys. Rev. Lett. **94**, 126802 (2005).
[8] H. Malissa, W. Jantsch, G. Chen, H. Lichtenberger, T. Fromherz, F. Schäffler, G. Bauer, A. Tyryshkin, S. Lyon, and Z. Wilamowski, in *Physics of Semiconductors: 28th Int. Conf. Phys. Semicond.*, edited by W. Jantsch and F. Schäffler, AIP Conf. Proc. No. 893 (AIP, New York, 2007), p. 1317.
[9] W. Jantsch, Z. Wilamowski, N. Sandersfeld, M. Mühlberger, and F. Schäffler, Physica E (Amsterdam) **13**, 504 (2002).
[10] Z. Wilamowski, W. Jantsch, H. Malissa, and U. Rössler, Phys. Rev. B **66**, 195315 (2002).
[11] Z. Wilamowski and W. Jantsch, Phys. Rev. B **69**, 035328 (2004).
[12] Y. Kato, R. C. Myers, A. C. Gossard, and D. D. Awschalom, Nature (London) **427**, 50 (2004).
[13] M. Schulte, J. G. S. Lok, G. Denninger, and W. Dietsche, Phys. Rev. Lett. **94**, 137601 (2005).
[14] W. Ungier, W. Jantsch, and Z. Wilamowski, Acta Phys. Pol. A **112**, 345 (2007).
[15] M. Duckheim and D. Loss, Nat. Phys. **2**, 195 (2006).
[16] M. I. Dyakonov and V. I. Perel, Sov. Phys. Solid State **13**, 3023 (1972).
[17] E. L. Ivchenko, Fiz. Tverd. Tela (Leningrad) **15** (5), 1566 (1973) [Sov. Phys. Solid State **15**, 1048 (1973)].
[18] Z. Wilamowski and W. Jantsch, Physica E (Amsterdam) **10**, 17 (2001).
[19] Yu. L. Bychkov and E. I. Rashba, J. Phys. C **17**, 6039 (1984).
[20] P. Pfeffer and W. Zawadzki, Phys. Rev. B **68**, 035315 (2003).
[21] P. Pfeffer and W. Zawadzki, Phys. Rev. B **74**, 115309 (2006).
[22] V. K. Kalevich and V. L. Korenev, Zh. Eksp. Teor. Fiz. **52**, 859 (1990) [JETP Lett. **52**, 230 (1990)]; Appl. Magn. Reson. **2**, 397 (1991).
[23] See e.g., C. P. Slichter, in *Principles of Magnetic Resonance*, Springer Series in Solid-State Sciences Vol. 1, 2nd ed., edited by M. Cardona, P. Fulde, and H.-J. Queisser (Springer-Verlag, Berlin, 1978).
[24] A. Abragam, *The Principles of Nuclear Magnetism* (Clarendon, Oxford, 1961), p. 41.
[25] G. Feher, A. F. Kip, and F. J. Dyson, Phys. Rev. **98**, 337 (1955).
[26] Z. Wilamowski, W. Jantsch, N. Sandersfeld, M. Mühlberger, F. Schäffler, and S. Lyon, Physica E (Amsterdam) **16**, 111 (2003).
[27] Junya Matsunami, Mitsuaki Ooya, and Tohru Okamoto, Phys. Rev. Lett. **97**, 066602 (2006).